Sensitized Luminescence of Lanthanides within the Walls of Polyethylenoxa-Pillared γ-Zirconium Phosphate

Ernesto Brunet,* María José de la Mata, Olga Juanes, and Juan Carlos Rodríguez-Ubis

Departamento de Química Orgánica, Facultad de Ciencias, C-1, Universidad Autónoma de Madrid, 28049 Madrid, Spain

Received December 11, 2003. Revised Manuscript Received February 11, 2004

Pillared γ-zirconim phosphate at low level with a diphosphonic acid resulting from the addition of pentaethyleneglycol to diethyl vinyl phosphonate was prepared and used as a porous matrix to intercalate $LnCl_3$ (Ln = Eu, Tb) and 2,2-bipyridyl (bpy). The uptake levels of both species in mild conditions were 0.35 and 0.10 equivalents per Zr, respectively. Strong interactions between the lanthanide ion and the polyethylenoxa chains were evidenced. Although powder XRD of the composite showed two interlayer distances (1.7 and 2.2 nm) indicating that the material was not homogeneous, excitation luminescence spectra confirmed strong lanthanide bpy-sensitized emission which was more than 50 times higher than that in nonpillared γ-zirconium phosphate.

Introduction

The use of solid matrixes as inorganic salts of tetravalent metals leads to well-organized materials where organic molecules with different functions may be grafted in an orderly manner.[1] In the so-called γ-ZrP [$Zr(PO_4)(H_2PO_4)\cdot 2H_2O$], the acidic phosphates exposed in the surface of the lamellae can be topotactically replaced by organic diphosphonic acids.[2] This is a simple way to obtain pillared organic−inorganic materials with high, controlled porosity.[3] Luminophores can thus be attached to these scaffolds to render solid, insoluble, and stable composite materials to be used in various applications such as optical nanodevices, sensors, data storage, etc.[4]

We are currently involved in the study of efficient lanthanide sensitization methods[5] and in the building of pillared, highly porous materials based on zirconium phosphate. Although some research has been performed on the intercalation of lanthanide complexes into α-ZrP[6] or γ-ZrP/phosphite,[7] there is no report of such studies on pillared γ-ZrP.

We have exchanged γ-ZrP at a low level with a diphosphonic acid derived from pentaethyleneglycol. Yet, instead of intercalating a preformed lanthanide chelate, we wanted to explore whether the pillared framework is able to provide the metal with the necessary conditions to display reasonable luminescence properties and minimize nonradiative deactivation pathways. Therefore, we have intercalated simple Ln^{3+} salts (Ln = Eu, Tb) within the large pores of the resulting polyethylenoxa pillared structure in order to study how the emission properties of the metal are affected in the presence or absence of simple metal sensitizers such as 2,2′-bipyridine (bpy).[8] In these conditions, even direct excitation of Ln^{3+} rendered a reasonable level of emission of the metal. However, when bpy was additionally intercalated in the pores of the pillared framework, Ln^{3+} displayed sensitized luminescence ("antenna effect" of bpy[9]) and metal emission increased dramatically. We hereby report the results of these experiments.

Experimental Section

General. MAS ^{31}P NMR spectra were recorded in a Bruker MSL 400 spectrometer (Instituto de Ciencias de Materiales CSIC, Madrid). Elemental analyses were performed in a Perkin-Elmer series II 2400 CHN analyzer (SidI, UAM). Powder XRD spectra were run in a Siemens D-5000 diffractometer (SidI, UAM) using Cu Kα radiation with Ni filter (40 kV, 30 mA). Thermogravimetric analyses (TGA) were carried out in a Mettler Toledo TGA/SDTA 851^e thermo balance at 5 °C/min. Luminescence spectra were recorded in the solid state in a Perkin-Elmer LS-50 spectrofluorimeter with a red-

* To whom correspondence should be addressed. E-mail: ernesto.brunet@uam.es.

(1) Brunet, E.; de la Mata, M. J.; Juanes, O.; Rodríguez-Ubis, J. C. *Angew. Chem., Int. Ed.* **2004**, *43*, 619.

(2) Clearfield, A.; Poojary, D. M. *J. Chem. Soc., Dalton Trans.* **1995**, 111.

(3) Brunet, E.; Huelva, M.; Vázquez, R.; Juanes, O.; Rodríguez-Ubis, J. C. *Chem. Eur. J.* **1996** *12*, 1578.

(4) Corriu, R. J. P.; Embert, F.; Medí, A.; Reyé, C. *Chem. Mater.* **2001**, *13*, 4542. Corriu, R. J. P.; Embert, F.; Guari, Y.; Mehdi, A.; Reyé, C. *Chem. Commun.* **2001**, 1119. Liu, Y.; Yu, G.; Wu, X.; Zhu, D. *Chem. Mater.*, **2000**, *12*, 2537. Tissue, B. M. *Chem. Mater.* **1998**, *10*, 2837. Parker, D.; Blair, S.; Lowe, M. P.; Mathieu, C. E.; Sennayake, P. K.; Kataky, R. *Inorg. Chem.* **2001**, *40*, 5860. Verhoeven, J. W.; Bakker, B. H.; Goes, M.; Hoebe, N.; van Ramesdonk, H. J.; Werts, M. H. V.; Hofstraat, J. W. *Coord. Chem. Rev.* **2000**, *208*, 3. Legendziewicz, J.; Maruszewski, K.; Strek, W.; Sokolnicki, J.; Reisfield, R.; Pavich, T. *Opt. Mater.* **1999**, *13*, 41. Ober, C. K.; Beecroft, L. L. *Chem. Mater.* **1997**, *9*, 1302.

(5) See for example Brunet, E.; Juanes, O.; Sedano, R.; Rodríguez-Ubis, J. C. *Org. Lett.* **2002**, *4*, 213. Alonso, M.; Brunet, E.; Juanes, O.; Rodríguez-Ubis, J. C. *J. Photochem. Photobiol.* **2002**, *147* (2), 113.

(6) Xu, R.; Xu, Q.; Fu, L.; Li, L.; Zhang, H. *J. Mater. Chem.* **2000**, *10*, 2532.

(7) Shakshooki, S. K.; El Hanash, H. B.; El-Mehdawi, R. M.; El-Mellah, M. A.; Arafa, E. A.; Bejey, A. M. *J. Radioanal. Nucl. Chem.* **1999**, *240*, 433.

(8) For studies on the intercalation of 2,2-bipyridil in γ-ZrP see Ferragina, C.; Cafarelli, P.; De Stefanis, A.; Mattei, G. *Mater. Res. Bull.* **1999**, *34*, 1039.

(9) Lehn, J. M.; Alpha, B.; Mathis, G. *Angew. Chem., Int. Ed. Engl.* **1987**, *26*, 266. Lehn, J. M.; Alpha, B.; Balzani, V.; Perathoner, S.; Sabbatini, N. *Angew. Chem., Int. Ed. Engl.* **1987**, *26*, 1266. Lehn, J. M.; Alpha, B.; Blasse, G.; Dirksen, G. J.; Sabbatini, N.; Perathoner, S. *J. Phys. Chem.* **1988**, *92*, 2419.

10.1021/cm0353106 CCC: $27.50
Published on Web 03/20/2004

Table 1. Characterization Data of Material I

equiv acid[a]/Zr	[Aacid] (mM)	%C obs. (calc.)[b]	%H obs. (calc.)[b]	x[c]	150−350°C (calc.)[d]	25−150°C	z[e]	d condit.[f]	d wet[g]	d (calc.)[h]
0.4	15	6.53 (6.6)	2.07 (2.1)	0.13	7.7 (6.2−9.8)	6.1	0.8	1.31	1.76	2.5

[a] See Scheme 1 and empirical formula: $\mathbf{Zr(PO_4)(H_2PO_4)_{1-2x}[C_6H_{16}O_8P_2(C_2H_4O)_4]_x \cdot zH_2O}$. [b] Elemental analysis. [c] Exchange level deduced from elemental analysis and liquid ^{31}P NMR in HF/DMSO-d_6. [d] Weight loss for polyethyleneglycol elimination reactions calculated from the exchange level deduced from elemental analysis and liquid ^{31}P NMR in HF/DMSO-d_6. [e] Water content determined by TGA and elemental analysis in conditioned samples. [f] Powder XRD interlayer distance (nm) measured in conditioned samples over $BaCl_2$ (90% r.h.). [g] Powder XRD interlayer distance (nm) measured just after centrifugation of samples. [h] Expected interlayer distance (nm) for the exchanged γ-ZP with the pentaethylenoxa diphosphonate pillar in helicoidal conformation.

sensitive Hamamatsu R-928 photomultiplier. X-ray total reflection fluorescence was performed in a Seifert EXTRA-II spectrometer with Si(Li) detector, 80-mm^2 active area, and resolution of 157 eV and 5.9 keV (Mn Kα). Computer modeling was performed with the HyperChem program.[10]

3,6,9,12,15,18-Hexaoxaeicosyl-1,20-diphosphonic acid (PEGDP). To a suspension of 1.1 g (3.2 mmol) of Cs_2CO_3 in 5 mL (32.5 mmol) of diethylvinylphosphonate at 90 °C under Ar, 0.62 g (2.6 mmol) of pentaethyleneglycol in 4−5 portions wete added over a period of 2−4 days and the disappearance of the latter was followed by TLC. When the glycol persisted, the reaction mixture was allowed to cool, treated with water (10 mL), and extracted with CH_2Cl_2 (3 × 20 mL). Usual workup of the extracts yielded a yellowish oil whose components (diphosphonate, $R_f = 0.6$; monophosphonate, $R_f = 0.5$) were separated by flash chromatography (CH_2Cl_2/EtOH 10:1). The separated diethyl pentaethylenoxa diphosphonate was dissolved in the sufficient amount of 35% HCl and the resulting solution was maintained at 90 °C overnight. The reaction mixture was dried under vacuum and the residue was used without further purification. Overall yield was 45%. ^{1}H NMR (D_2O) δ (ppm): 3.54 (m, 24H, CH_2OCH_2); 1.93 (dt, $J = 7.7$ Hz, $J_{HP} = 18.6$ Hz, 4H, PCH_2CH$_2$O). ^{13}C NMR (D_2O) δ (ppm): 70.1 (PCH$_2$CH$_2$OCH$_2$CH_2); 69.8 (PCH$_2$CH$_2$OCH_2); 65.4 (PCH$_2$CH_2O); 27.8 (d, $J = 134.5$ Hz, CH_2P). MS (L − SIMS$^+$): 455.1 (M + H$^+$, 100); 477.1 (M + Na$^+$, 22); 909.2 (2M + H$^+$, 2). Elemental analysis calculated for $C_{14}H_{32}P_2O_{12}\cdot 4H_2O$: C, 31.94; H, 7.66. Observed: C, 31.72; H, 7.49.

Topotactic Exchange of PEGDP on γ-ZP. The inorganic γ-ZP phase (1 g) was dispersed in a 1:1 deionized water/acetone mixture (100 mL) at 80 °C. The suspension was kept for 20 min in a stoppered bottle to attain complete exfoliation. The appropriate amount of PEGDP (see Table 1) was dissolved in a 1:1 deionized water/acetone mixture (50 mL per mmol of acid) and the solution was then added at 80 °C to the exfoliated γ-ZP phase. The resulting dispersion was kept at 80 °C overnight, allowed to cool, and centrifuged. The white solid was decanted and washed/centrifuged with deionized water (3 × 20 mL). The wet material was dried for 24 h at 100 °C and subsequently conditioned to 90% r.h. ($BaCl_2$).

Intercalation of Ln^{3+}. The starting solid phase (0.2 g) was suspended in 20 mL of a 0.1 M aqueous solution of $LnCl_3$ (Aldrich). The suspension was stirred at room temperature for 48 h. The solid was then centrifuged, washed/centrifuged with deonized water (3 × 20 mL), and dried at 100 °C for 3 h.

Intercalation of 2,2′-Bipyridyl. The starting solid phase (0.2 g) was suspended in 20 mL of a 0.1 N solution of 2,2′-bipyridyl (Aldrich) in ethanol. The suspension was stirred at room temperature for 48 h. The solid was then centrifuged, washed/centrifuged with ethanol (2 × 20 mL) and deonized water (2 × 20 mL), and dried at 100 °C for 3 h.

Results and Discussion

Synthesis of pentaethyleneglycol-derived diphosphonic acid (3,6,9,12,15,18-hexaoxaeicosyl-1,20-diphosphonic acid; **1**) and the pillaring procedure by means of its topotactic exchange into γ-ZrP were performed as indicated in the Experimental Section (Scheme 1).[11]

(10) Hypercube, Inc. 1115 NW 4th Street, Gainesville, FL 32601.

Scheme 1. Synthetic Path Leading to Material I

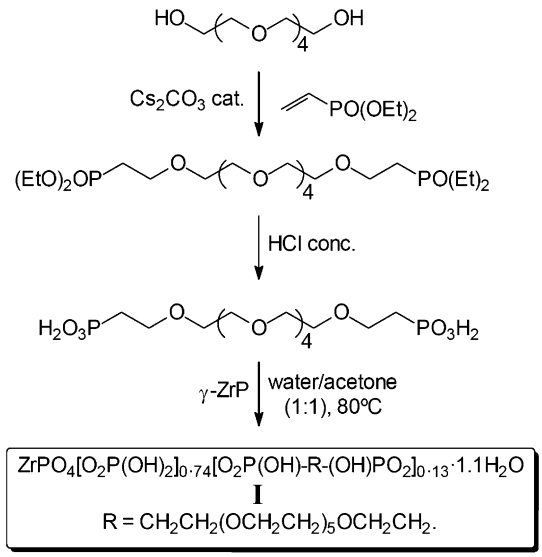

We thus obtained material **I** for which elemental analysis, TGA, and NMR studies (Table 1) gave an empirical formula of $ZrPO_4[O_2P(OH)_2]_{0.74}[O_2P(OH)\text{-}R\text{-}(OH)PO_2]_{0.13}\cdot 1.1\ H_2O$ where R = $CH_2CH_2(OCH_2CH_2)_5OCH_2CH_2$.

Figure 1 shows the MAS ^{31}P NMR spectrum of **I** which exhibits three signals at chemical shifts −27.1 (PO_4), −13.6 [$O_2P(OH)_2$], and 15.8 [$O_2P(OH)$-R-(OH)-PO_2] ppm of relative intensity 1:0.69:0.25 in excellent accordance with the calculated empirical formula. Under typical cross-polarization conditions (contact time 2 ms), the signals at −13.6 and 15.8 ppm suffered heavy intensity increments (Figure 1) as expected from their proximity to hydrogen atoms either from the acid phosphates, the organic chain, or the interlayer water molecules.

FT-IR spectra of **I** showed new absorptions in the fingerprint region at 1353 and 1311 cm^{-1}, not seen in γ-ZrP, which were respectively attributed to the wag-

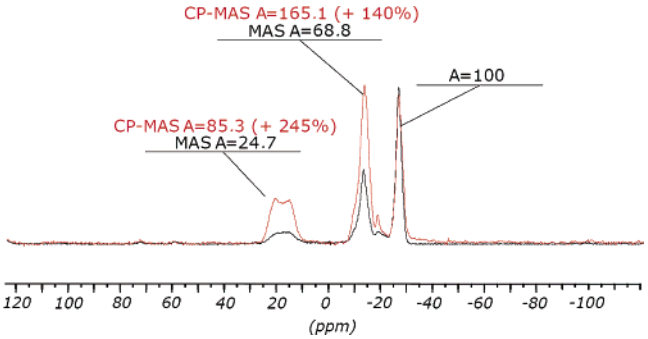

Figure 1. Solid-state ^{31}P NMR spectra of material **I**.

Table 2. Results of $LnCl_3$ Intercalation into Pillared Material I (Scheme 1) and γ-ZrP

material[a]	x[b]	y[b]	n[c]	d (nm)[d]
γ-ZrP−**Eu**	0.22	0.22	2.1	1.24
γ-ZrP−**Tb**	0.15	0.14	2.1	1.24
I−Eu	0.35	0.25	2.4	1.72
I−Tb	0.33	0.17	2.4	1.62

[a] **γ-ZrP-Ln**: $ZrPO_4(H_{2-3x+y}PO_4)(Ln)_xCl_y{\cdot}nH_2O$. **I-Ln**: $ZrPO_4(H_{2-3x+y}PO_4)_{0.74}(\mathbf{1})_{0.13}(Ln)_xCl_y{\cdot}nH_2O$. [b] Measured by X-ray total reflection fluorescence. [c] TGA analysis. [d] Measured by powder XRD.

Table 3. Interlayer Distances of γ-ZrP Intercalated with Different Cations

cation	d (nm)[a]
none	1.72
$MeNH_3^+$	2.70
Li^+	2.52
Na^+	2.54
Cs^+	2.51
Eu^{3+}	1.72
Tb^{3+}	1.62

[a] Measured by powder XRD.

ging and torsion bands of the $O-CH_2-CH_2-O$ fragments in gauche conformation,[12] suggesting that the pentaethylenoxa chains adopt helicoidal arrangements. However, the maximum interlayer distance calculated for the helicoidal arrangement of perpendicular pillars (2.5 nm) is far from being reached even in wet samples of **I** (Table 1), thus showing that the organic columns remain more or less parallel to the layers, depending on the humidity level, probably interacting with the superficial acidic phosphates by hydrogen-bonding interactions. Yet, the pillared structure of **I** was put out of question by the discovery of its accordion-like behavior that was previously described by us elsewhere.[8]

Treatment of **I** with aqueous 0.1 M $LnCl_3$ led to partial H^+/Ln^{3+} exchange, with some chloride atoms remaining as counterions. Table 2 compares pertinent data concerning Ln^{3+} uptake of pillared **I** and plain γ-ZrP.

Three main evidences indicate that the polyethylenoxa pillars strongly interact with the Ln^{3+} cations. First, it should be noted that in the very same intercalation conditions, the uptake of Ln^{3+} by bare γ-ZrP was almost half that of **I**, despite the large volume of the interlayer region that the polyethylenoxa pillars should be occupying. The second evidence may be visualized from Table 3, which shows interlayer distances of **I** measured by powder XRD when different cations were intercalated by simple acid−base titrations.

With alkaline cations or small amines, interlayer distance jumps ca. 0.8−1.0 nm. This reversible phenomenon allowed us to describe for the first time what we designated as chemical accordion-like movement, and, as it was mentioned earlier, this is the key evidence to the true pillared nature of **I**. However, in contrast with the other cations, Ln^{3+} uptake did not cause interlayer distance to increase but even caused it to shrink 0.1 nm in the case of Tb^{3+}. The strong oxygenophilicity of lanthanide cations should make it interact

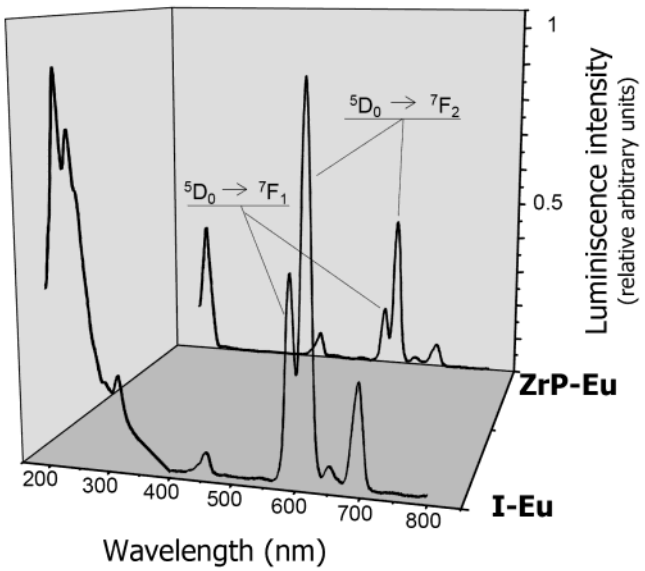

Figure 2. Excitation−emission spectra of the indicated materials.

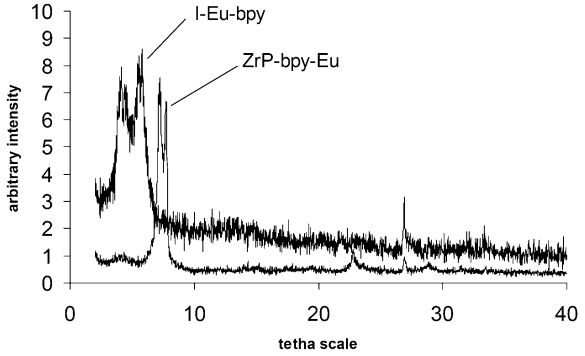

Figure 3. Powder XRD spectra of the indicated materials.

with as many oxygens as possible from either the superficial exchangeable phosphates or the polyethyleneoxa chains, thus forcing the latter to be as close as possible to the surface of the inorganic layer.

The last fact evidencing the strong influence of the polyethylenoxa pillars over Ln^{3+} cations comes from luminescence studies. Figure 2 shows the excitation−emission spectra of **γ-ZrP−Eu** and **I−Eu** materials.

We indicated above that the Eu^{3+} uptake levels (*x* in Table 2) were 1.6 times higher in **I**. In turn, it can be deduced from Figure 2 that emission intensity was raised by a factor of 2.4 when Eu^{3+} resided in the pillared material. Besides, emission lifetimes were 0.50 and 0.72 ms in **γ-ZrP−Eu** and **I−Eu**, respectively. Although direct excitation of the metal is a very inefficient method to obtain its luminescence, the higher intensity and longer emission lifetimes displayed by **I−Eu** are an indisputable sign of higher emission efficiency in the pillared material. It should be noted that one common pathway of undesired lanthanide deactivation is the coupling of excited states with water O−H oscillators. TGA studies revealed that water content of **I−Eu** was even a bit higher than that of **γ-ZrP−Eu** (Table 2) but the former showed better emission properties, thus suggesting that the polyethylenoxa pillars play a decisive role in encapsulating the metal. This is also suggested by the decrease in the relative intensity of the indicated Eu transitions in

(11) Alberti, G.; Brunet, E.; Dionigi, C.; Juanes, O.; de la Mata, M. J.; Rodríguez-Ubis, J. C. Vivani, R. *Angew. Chem., Int. Ed.* **1999**, *38*, 3351.

(12) Begum, R.; Matsuura, H. *J. Chem. Soc., Faraday Trans.* **1997**, *93*, 3839.

Table 4. Results for the Two Possible Orders of Intercalation of $EuCl_3$ and bpy into Pillared Material I (Scheme 1) and γ-ZrP

		resulting material					
starting material	starting *x* or *z*[a]	*x*[b]	*y*[b]	*z*[c]	*n*[d]	*d*[e]	acronym
γ-ZrP−Eu	*x* = 0.22	0.18	0.01	0.03	2.0		
I−Eu	*x* = 0.35	0.35	0.27	0.10	2.3	1.7, 2.2	**I**−Eu-bpy
γ-ZrP−bpy	z = 0.13	0.10	0.09	0.10	1.2	1.1, 1.2	γ-ZrP−bpy-Eu
I−bpy	z = 0.17	0.28	0.07	0.02	3.0		

[a] Sub index *x* in: **γ-ZrP−Eu**, $ZrPO_4(H_{2-3x+y}PO_4)(Ln)_xCl_y{\cdot}nH_2O$; **I−Eu**, $ZrPO_4(H_{2-3x+y}\ PO_4)_{0.74}(\mathbf{1})_{0.13}(Ln)_xCl_y{\cdot}nH_2O$. Sub index *z* in: **γ-ZrP−bpy**, $ZrPO_4(H_2PO_4)(bpy)_z{\cdot}nH_2O$; **I−bpy**, $ZrPO_4(H_2PO_4)_{0.74}(\mathbf{1})_{0.13}(bpy)_z{\cdot}nH_2O$. [b] Measured by X-ray total reflection fluorescence. [c] Measured by elemental analysis. [d] Measured by TGA analysis. [e] Measured by powder XRD (Figure 3).

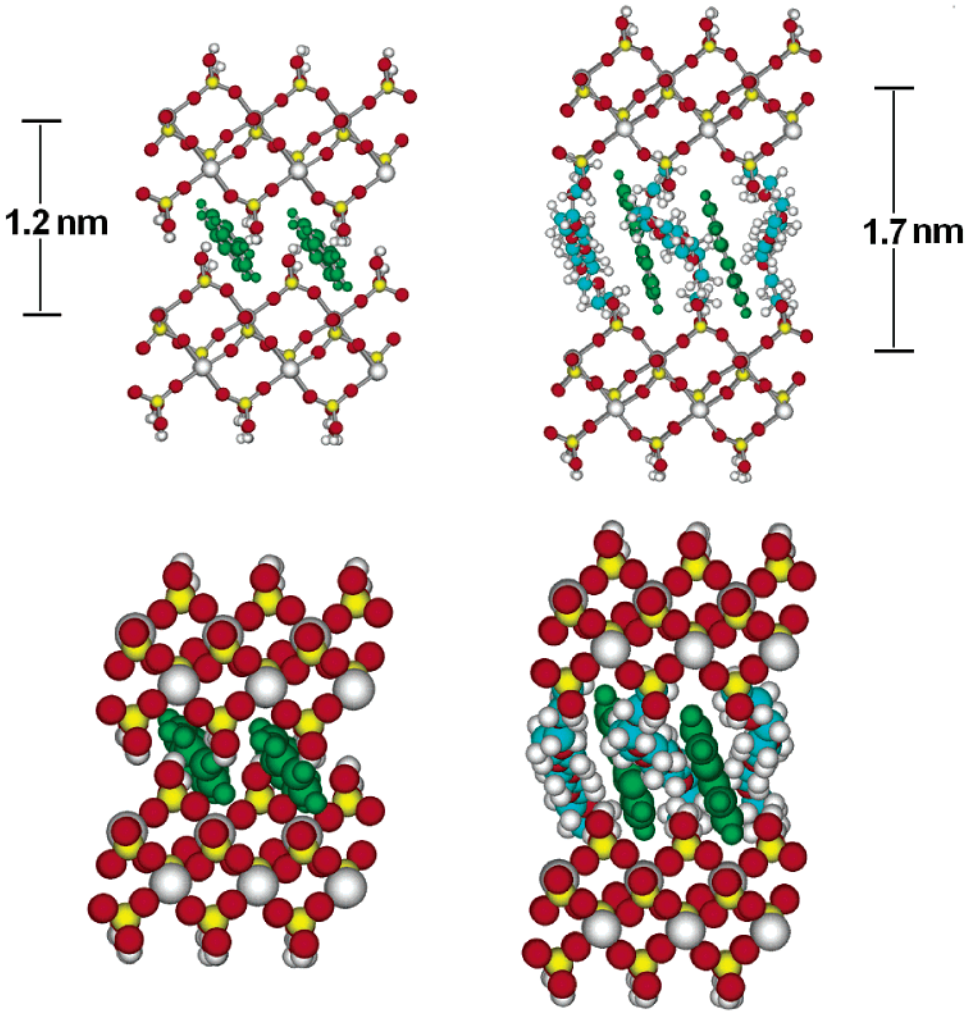

Figure 4. Calculated model structures for **γ-ZrP-bpy** (left) and **I-bpy** (right).

Figure 2 ($^5D_0-{}^7F_2/{}^5D_0-{}^7F_1$) from **γ-ZrP−Eu** (2.64) to **I−Eu** (1.85) that hints to higher order in the surroundings of the metal in **I−Eu**.[13] On the other hand, excitation spectra of **I−Eu** showed new bands (240, 313 nm; cf. Figure 2) as compared to that of **γ-ZrP−Eu** (222 nm) indicating that the coordination sphere of the metal is quite different in both materials.[14]

The behavior of Tb^{3+} deserves less comment because its emission spectrum is not as sensitive as that of Eu^{3+} to environmental changes.[12] However, although Tb^{3+} showed a lower emission intensity increase (1.5) from **γ-ZrP−Tb** to **I−Tb**, the increase of its lifetime (2.01 and 2.61 ms, respectively) also indicates a favorable interaction of the polyethylenoxa pillars with this cation.

A striking response was obtained when a chromophore as simple as 2,2′-bipyridyl (bpy) was intercalated into **I-Ln**. There are two obvious possibilities in the order of intercalation of Ln and bpy into **γ-ZrP** and **I**. Table 4 shows that they were not equivalent in the case of Eu^{3+} cations.[15]

The higher intercalation values for both metal and bpy were obtained for **I** when the order of intercalation

(13) Richardson, F. S. *Chem. Rev.* **1982**, *82*, 541.

(14) Phenomena as rigidochromism observed for transition metals (see for example Itokazu, M. K.; Polo, A. S.; Iha, N. Y. M. *J. Photochem. Photobiol. A* **2003**, *160*, 27−32) or ion clustering and segregation observed in glasses (de Graaf, D.; Stelwagen, S. J.; Hintzen, H. T.; de With, G. *J. Non-Cryst. Solids* **2003**, *325*, 29−33) are out of the scope of this work and have not been addressed.

(15) Since results for Tb^{3+} were similar they have been omitted for the sake of brevity.

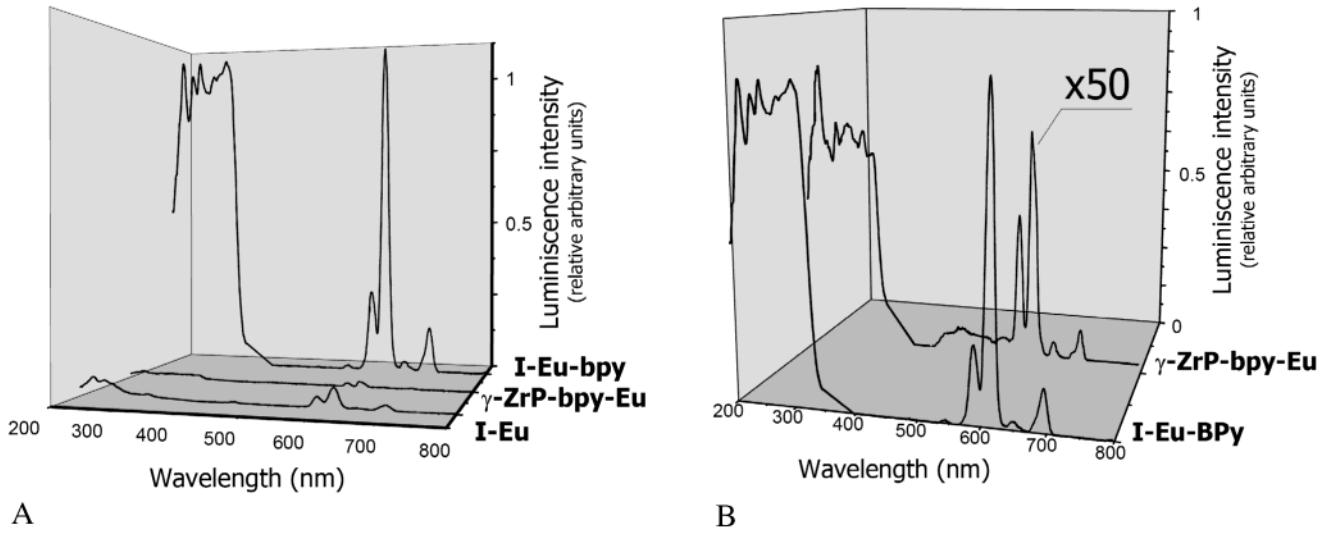

Figure 5. A: Excitation−emission spectra of the indicated materials. B: Vertical expansion (×50) of **γ-ZrP-bpy-Eu** spectrum as compared to unexpanded **I−Eu-bpy**.

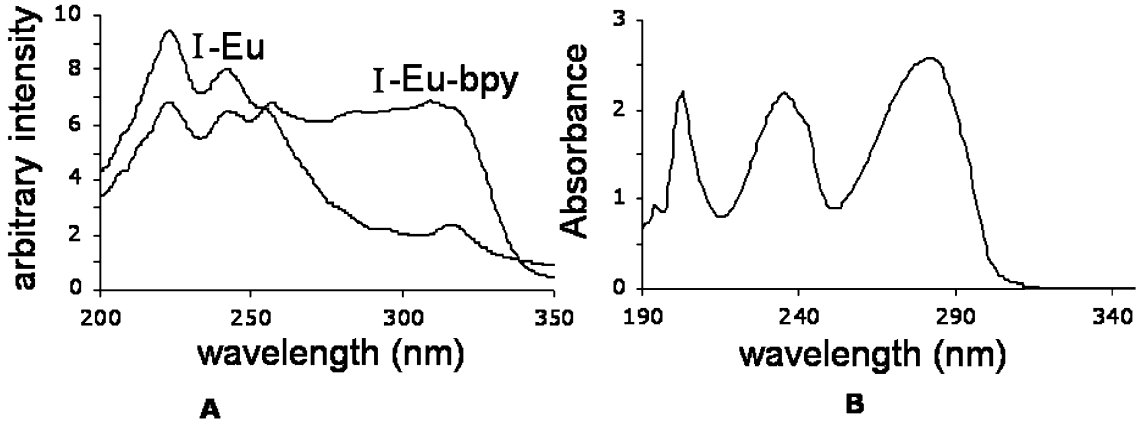

Figure 6. A: Excitation spectra of the indicated materials (trace of **I−Eu** ×25; monitored wavelength 617 nm). B: Absorption spectrum of 2,2-bipyridil in ethanol solution.

was metal first, bpy second, whereas the opposite was true for **γ-ZrP**. XRD spectra showed that **I−Eu-bpy** had low crystallinity, and two broad interlayer spacing peaks were discernible at 2θ angles corresponding to 1.7 and 2.2 nm (Figure 3). Whether the first distance corresponds to the initial phase (cf. Table 2) or bpy intercalation led to two different intercalates remains uncertain. At the least, part of the **I−Eu** phase expanded 0.44 nm to admit the incorporation of bpy. The phase **γ-ZrP-bpy-Eu** also showed two peaks (Figure 3) corresponding to interlayer spacings of 1.1 and 1.2 nm, very similar to the initial, short distance measured in **γ-ZrP−Eu** (Table 2).

Molecular modeling (Figure 4) suggests that even a pillared phase with layers separated by 1.1−1.2 nm bears empty pockets of enough size to enshroud bpy molecules. On the other hand, the observed uptake level of bpy (ca. 10%; *z* in Table 4) is much higher than that expected (0.5−1%) if the incorporation of the heterocycle would have only happened in the surface of a typically sized particle (Coulter method, 0.5−2 μm).[16] These data indicate that although materials **I-Ln-bpy** and **γ-ZrP-bpy-Ln** do not appear to be highly homogeneous, the major part of their active components are truly entrapped in the inorganic layers.

Figure 5 shows the excitation−emission spectra of the indicated materials and the substantial increase of Eu^{3+} emission in the pillared material **I−Eu-bpy**.[13] From Figure 5A the importance of the pillaring is made evident. The intensity of emission for **γ-ZrP-bpy-Eu**, with no pillars but having the sensitizer, is even lower than that of the pillared **I−Eu** but without sensitizer. Figure 5B shows that, in the very same conditions of measurement, the emission of **I−Eu-bpy** was more than 50 times superior to that of **γ-ZrP-bpy-Eu**. This is too high a factor to be explained solely by the fact that **I−Eu-bpy** holds 3.5 times as much metal as **γ-ZrP-bpy-Eu** (cf. *x* in Table 4).

Figure 6A compares the excitation spectra of **I−Eu** and **I−Eu-bpy** and 6B shows the UV spectrum of bpy in ethanol solution. The strong absorption of bpy at 285 nm suggests that the broad band in the range of 280−330 nm displayed by **I−Eu-bpy** in its excitation spectrum corresponds to bpy sensitization. This evidence supports that bpy is exerting the expected antenna effect in **I−Eu-bpy**.

(16) See for example Alberti, G.; Dionigi, C.; Giontella, E.; Murcia-Mascarós, S.; Vivani, R. *J. Colloid Interface Sci*, **1997**, *188*, 27. Ferragina, C.; Massucci, M. A.; Patrono, P.; Ginestra, A.; Tomlinson, A. A. G. *J. Chem. Soc., Dalton Trans.* **1988**, 851.

It should be noted that the excitation profiles of pillared **I**−**Eu-bpy** and nonpillared γ-**ZrP-bpy-Eu** (Figure 5B) are very similar, implying that bpy plays the sensitizer role in both materials. However, the much higher emission intensity achieved in **I**−**Eu-bpy** points to a very special importance of the polyethylenoxa pillars in making the interlayer space adequate for bpy to transfer energy to Eu^{3+} much more efficiently. Powder XRD (Table 4) evidenced that the layers in **I**−**Eu-bpy** are much further apart (1.7−2.2 nm) than those in γ-**ZrP-bpy-Eu** (1.1−1.2 nm). Figure 4 presents drawings of calculated models showing possible arrangements of intercalated 2,2′-bipyridyl. It can be easily seen that bpy is quite constricted in γ-**ZrP-bpy-Eu**, whereas the pillared structure of **I**−**Eu-bpy** (even that of the shortest interlayer distance) allows for the intercalated molecule to have much more available space and consequently more degrees of freedom. This could explain the low crystallinity observed in XRD for the latter (see above). In these conditions, the sensitizer in **I**−**Eu-bpy** can adopt, at least in average, satisfactory orientations relative to the metal in order to efficiently pass energy to it. It should be remarked that the ratio $^5D_0-^7F_2/^5D_0-^7F_1$ (cf. Figure 5B) is nevertheless higher in **I**−**Eu-bpy** (4.72) than in γ-**ZrP-bpy-Eu** (1.57) thus showing that the order around the metal is lower in the pillared material. This is a clear indication that an ordered metal environment is not a decisive factor to achieve effective lanthanide sensitization.

As a final conclusion, this work evidences that pillared γ-ZrP with polyoxygenated chains, as simple as those derived from polyethyleneglycols, may constitute a good housing for the sensitized emission of lanthanides, thus paving the road to the synthesis of highly luminescent solids for applications in optical devices. Much work is in progress to improve the properties and homogeneity of the pillared intercalates.

Acknowledgment. Financial support from Comisión Interministerial de Ciencia y Tecnología of Spain (CICYT; grant MAT02-03243) and indirect funding from FYSE-ERCROS S.A. are gratefully acknowledged.

CM0353106